Research Article Vol. 61, No. 3 / 20 January 2022 / Applied Optics 837

applied optics

Inter-spacecraft offset frequency setting strategy in the Taiji program

Jiafeng Zhang,[1,2] Zhen Yang,[1] Xiaoshan Ma,[1,*] Xiaodong Peng,[1,3] Heshan Liu,[4] Wenlin Tang,[1] Mengyuan Zhao,[1,2] Chen Gao,[1] Li.-E. Qiang,[1] Xiaoqing Han,[1,2] and Binbin Liu[1,2]

[1]Key Laboratory of Electronics and Information Technology for Space System, National Space Science Center, Chinese Academy of Sciences, Beijing 100190, China
[2]University of Chinese Academy of Sciences, Beijing 100049, China
[3]School of Fundamental Physics and Mathematical Sciences, Hangzhou Institute for Advanced Study, UCAS, Hangzhou 310024, China
[4]National Microgravity Laboratory, Institute of Mechanics, Chinese Academy of Sciences, Beijing 100190, China
*Corresponding author: maxs@nssc.ac.cn

Received 8 September 2021; revised 16 December 2021; accepted 17 December 2021; posted 17 December 2021; published 20 January 2022

For controlling the beat frequency of heterodyne interferometry so that the Taiji program can detect gravitational waves in space, an offset frequency setting strategy based on a linear programming algorithm is proposed. Considering factors such as Doppler frequency shift, phase-locking scheme, laser relative intensity noise, and phase detector bandwidth, inter-spacecraft offset frequency setting results suitable for the Taiji program are obtained. During the six years of running the detection process, the use of frequency bounds in the range of [5 MHz, 25 MHz] showed that offset frequencies will remain unchanged for a maximum of 1931 days. If the upper and lower bounds are adjusted, and the relative motion between spacecraft is further constrained, the offset frequencies do not need to change during the time of the mission. These results may provide insights into selecting the phase detector and designing operation parameters such as orbit and laser modulation frequency in the Taiji program.

https://doi.org/10.1364/AO.442583

1. INTRODUCTION

In 2008, the Chinese Academy of Sciences began the "Taiji program" [1] aimed at performing space-based gravitational wave (GW) [2–4] detection in middle- and low-frequency bands [5]. This particular detection system uses a triangular formation comprising three spacecrafts (S/Cs). Each S/C follows a heliocentric orbit, and the distance between the S/Cs can reach millions of kilometers. Moreover, the disturbances in the curvature of the spacetime by GWs [2,6] can be observed using a laser interferometer ranging system [7,8]. A Doppler frequency shift is generated during a space GW detection mission due to the relative motion between S/Cs, which is related to choice of orbit [9,10]. Thus, heterodyne interferometry is used, and the beat frequency readout is varied over time. Due to the long-distance propagation and the finite receiving aperture, only very few fractions of the transmitted light from the remote S/C can be received by the local S/C, and the phase-locking scheme is adopted so that the local S/C operates as a "phase transponder" [11,12]. In particular, the local laser is controlled to track and lock the phase of the remote laser using the beat frequency information of the interference between lasers on the local and remote S/Cs. Subsequently, the local laser is emitted back to the remote S/C to achieve the purpose of light intensity amplification and phase information maintenance [13].

Within the above heterodyne interferometry system, various frequencies and frequency ranges must be avoided. First, the homodyne interference phenomenon that will lead to the inability to extract phase information is not allowed. Furthermore, the laser relative intensity noise (RIN) and phase detector bandwidth limit the minimum and maximum of the beat frequency. RIN is part of the read-out noise [14] of the receiving photodetector and comes from the fluctuations in the laser power relative to the average absolute power level. The lower bound of the beat frequency was set to 7 and 5 MHz in the laser interferometer space antenna (LISA) [15] and the evolved laser interferometer space antenna (eLISA) [16] missions, respectively [11]. Considering the suppression ability of intensity noise of the candidate laser for the Taiji program, this value is usually greater than 1.5 MHz [17] and is set to 5 MHz to obtain the best performance. The bandwidth of the phase detector determines the higher-frequency limit. According to the design parameter of the phase detector for the Taiji program, this value is approximately 25 MHz. However, the Doppler shift due to the inter-spacecraft motion varies with time; thus, the

beat frequency should be controlled within an allowable range during the detection process. There are two basic approaches of fixed beat frequencies and fixed laser offset frequencies to resolve the problem. Both methods have certain requirements for the relative motion speed of the orbit. The advantage of a fixed beat frequency is that it requires little bandwidth for a photodetector and phase detector; however, it needs to feed back the Doppler frequency to the laser, which makes the system more complex. At the same time, it is also difficult to calculate the Doppler frequency in data processing. In contrast, the fixed offset frequency method has the advantage of relatively simple data processing. The disadvantage is that there are certain requirements for the bandwidth of the photodetector and phase detector; further, the offset frequency needs to be optimized by an algorithm. According to the current technical progress, photodetectors and phase detectors have been able to meet the bandwidth requirements. In order not to increase the complexity of system and data processing, the fixed offset frequency has become a widely used method.

As mentioned, a crucial problem of the fixed offset frequency method is the reasonable planning of the offset frequency to ensure it remains fixed during scientific observation and even the whole mission cycle. Once the offset frequency changes, it needs to be modified by uploading instructions from the ground, and the interferometry needs to be restarted, which will inevitably lead to the interruption of observation data. The international LISA team realized the importance of this problem. The beat frequencies for both LISA and eLISA tasks were analyzed and designed [15,16,18,19]. Barke [11] applied a genetic algorithm (GA) to solve the problem for LISA and obtained a setting strategy. For instance, the offset frequencies theoretically did not require changing for a maximum of 177 days within the specified constraints. However, the optimization results were unstable because of the complexity and randomness of the GA. In this study, a linear programming (LP) algorithm is adopted to model and solve the setting strategy of the offset frequencies.

The remainder of this paper is organized as follows: Section 2 introduces the limiting factors of the beat frequency and selection of the phase-locking scheme. Section 3 uses the LP algorithm to solve the problem based on the selected phase-locking scheme. Finally, Section 4 discusses the effect of the maximum duration of offset frequencies under different frequency bounds and Doppler shifts.

2. LIMITATION OF BEAT FREQUENCY

During space GW detection, relative motion exists between the S/Cs, leading to the Doppler shift phenomenon. The relationship between the Doppler frequency shift and relative motion of the S/Cs is given as follows:

$$f_d = -\frac{v}{c} f_0, \tag{1}$$

where v represents the relative velocity between two S/Cs, c is the speed of light, and f_0 is the laser frequency.

Two laser beams from local and remote S/Cs generate the beat frequency via interference. The initial frequency of the two laser beams on the two S/Cs is f_0. Without frequency control, the laser frequency arriving at the local S/C from the remote S/C becomes $f_0 + f_d$ after a long-distance propagation. Following the interference of this laser with the local laser, the beat frequency signal f_d is generated. According to the fixed offset frequency method, an offset frequency Δf is added to control the beat frequency, and the laser frequency on the remote S/C is $f_0 + \Delta f$. Through transmission between the two S/Cs, the laser frequency becomes $f_0 + \Delta f + f_d$. Accordingly, the beat frequency produced by the interference with the local laser is $\Delta f + f_d$. By reasonably setting the value of offset frequency Δf, the beat frequency can satisfy the bandwidth requirement of the phase detector and effectively avoid low-frequency bands, in which the heterodyne signal will be submerged by the relative intensity noise of the laser.

A. Spacecraft Orbit Selection and Doppler Shift

The Taiji program entails three S/Cs that form an equilateral triangle. The orbital plane of the S/C constellation is initially set to an elliptical orbit with the sun as the center and an orbital period of one year. The space between them (arm length) is approximately 3 million km [1,5].

The key to detecting GWs lies in measuring the distance change caused by GWs using laser interferometry. After determining the S/C constellation shape and arm length, an appropriate orbit position should be selected to ensure the stability of the constellation. Constellation stability includes arm-length variation, arm-length variation rate, and angle variation between the two arms [10]. The design requirements of the Taiji program are listed in Table 1. The arm-length variation of the S/C formation should be less than 1% of the initial arm length of the S/C during the four to six years of operation. That is, the range should not exceed 3×10^4 km, the change rate of the arm length (or Doppler shift) should be less than ± 9 m/s, and the change in the angle between the two arms should be less than $\pm 1.5°$.

Tang [10] established a constellation orbit that satisfied the above constraints. The angle between the constellation plane and Earth was 23°. The constellation orbit diagram is shown in Fig. 1. During the six years of mission execution, the

Table 1. Orbit of the Taiji Program Design Requirements

Arm-Length Variation	Arm-Length Change Rate	Change in the Angle Between the Two Arms
$\leq 3 \times 10^4$ km	(−9 m/s, 9 m/s)	(−1.5°, 1.5°)

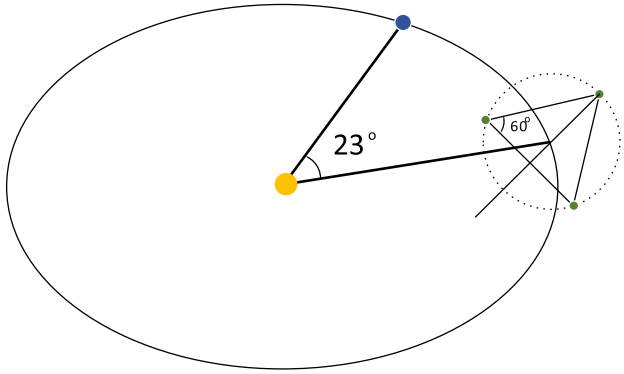

Fig. 1. Taiji spacecraft constellation orbit.

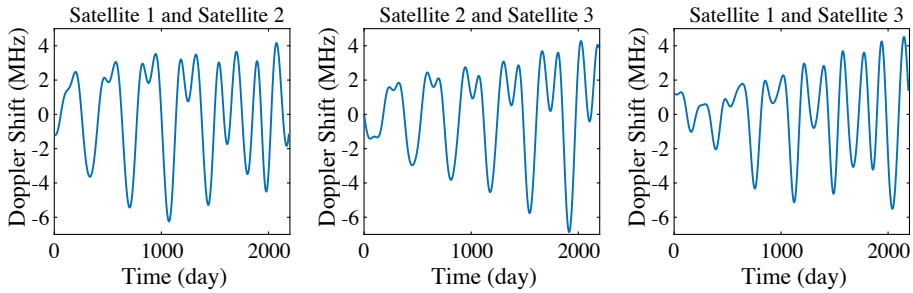

Fig. 2. Doppler shift among three spacecraft.

maximum arm-length change was less than 3×10^4 km, the maximum Doppler shift was less than 8 m/s, and the maximum angle change between the two arms was less than 0.5°. These values were obtained mathematically and through computer simulations. The Doppler shift among the three S/Cs of the constellation is shown in Fig. 2. Evidently, the inter-spacecraft Doppler frequency shift oscillation amplitude becomes increasingly larger over time and did not change periodically; further, the range of Doppler shift between each S/C exceeded 11 MHz, and the oscillations above and below 0 do not allow homodyne interference in the laser interference process in the Taiji program. Therefore, the beat frequency obtained via laser interference can easily exceed the bandwidth of the phase detector or be affected by the laser relative intensity noise.

B. Locking Scheme

The constellation of the Taiji program comprises three S/Cs, each with two lasers. A total of six laser links are formed. Moreover, a phase-locking loop is used to add an offset frequency to control the Doppler shift effect on the beat frequency. During the mission, the laser frequencies are locked to the adjacent laser frequency; in addition, only one laser is selected to be the master laser with a constant frequency, which is prestabilized by a reference cavity [5,20,21].

Because different phase-locking schemes will have different effects on the beat frequency, selecting an appropriate phase-locking scheme is necessary. Barke [11] conducted in-depth research on this subject, finding the phase-locking schemes suitable for the Taiji program. We chose the particular phase-locking plan shown in Fig. 3.

In Fig. 3, A, B, C, D, E, and F represent the six tunable lasers placed on three S/Cs, respectively. The laser frequency can be tuned by two ways: temperature tuning and piezoelectric transducer loaded on the laser crystal [17]. A and B are the two lasers in S/C 1, C and D are the two lasers in S/C 2, and E and F are the two lasers in S/C 3. Laser A is selected as the master laser. Δf^1_{AB} is the offset frequency between Laser A and Laser B in S/C 1. Similarly, Δf^2_{CD}, Δf^3_{EF}, Δf^1_{AF}, and Δf^1_{BC} are the offset frequencies between other lasers. The offset frequency can be planned to perform beat frequency control. Moreover, $f_{12}(t)$, $f_{13}(t)$, and $f_{23}(t)$ are the time-varying Doppler shifts.

This phase-locking scheme uses Laser A as the global reference system, and its frequency is set to a constant value f_0. Laser F is locked to Laser A, Laser B is locked to Laser A, Laser C is locked to Laser B, Laser D is locked to Laser C, and Laser E is locked to Laser F. Therefore, each laser's frequency after

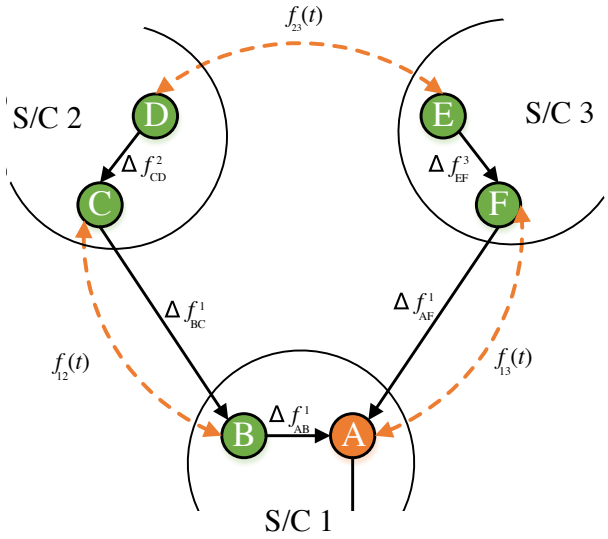

Fig. 3. Possible phase-locking scheme for space GW detection [11].

locking is calculated as shown in Eq. (2); each laser's modulation frequency Mf_i (i = A, F) by an optical phase lock loop is calculated by Eq. (3):

$$\begin{cases} f_A = f_0 \\ f_B = f_0 + f_{12}(t) + \Delta f^1_{AB} \\ f_C = f_0 + f_{12}(t) + \Delta f^1_{AB} + \Delta f^1_{BC} \\ f_D = f_0 + f_{12}(t) + \Delta f^1_{AB} + \Delta f^1_{BC} + \Delta f^2_{CD} \\ f_E = f_0 + f_{13}(t) + \Delta f^1_{AF} + \Delta f^3_{EF} \\ f_F = f_0 + f_{13}(t) + \Delta f^1_{AF} \end{cases}, \tag{2}$$

$$\begin{cases} Mf_A = 0 \\ Mf_B = f_{12}(t) + \Delta f^1_{AB} \\ Mf_C = f_{12}(t) + \Delta f^1_{AB} + \Delta f^1_{BC} \\ Mf_D = f_{12}(t) + \Delta f^1_{AB} + \Delta f^1_{BC} + \Delta f^2_{CD} \\ Mf_E = f_{13}(t) + \Delta f^1_{AF} + \Delta f^3_{EF} \\ Mf_F = f_{13}(t) + \Delta f^1_{AF} \end{cases}. \tag{3}$$

Thus, each inter-spacecraft beat frequency is calculated as follows:

$$\begin{cases} f^1_{\mathrm{het\_AF}} = \Delta f^1_{AF} + 2f_{13}(t) \\ f^1_{\mathrm{het\_BC}} = \Delta f^1_{BC} + 2f_{12}(t) \\ f^2_{\mathrm{het\_DE}} = \Delta f^1_{AF} + f_{13}(t) + \Delta f^3_{EF} + f_{23}(t) \\ \qquad\qquad -(\Delta f^1_{AB} + \Delta f^1_{BC} + f_{12}(t) + \Delta f^2_{CD}) \\ f^3_{\mathrm{het\_DE}} = \Delta f^1_{AF} + f_{13}(t) + \Delta f^3_{EF} \\ \qquad\qquad -(\Delta f^1_{AB} + \Delta f^1_{BC} + f_{12}(t) + \Delta f^2_{CD} + f_{23}(t)) \end{cases}. \tag{4}$$

3. OFFSET FREQUENCIES SETTING STRATEGY BASED ON LP

A. LP Modeling

A mathematical model based on LP was established according to the above orbit and phase-locking scheme. Offset frequencies can be planned using this model, such that the beat frequency of heterodyne interference is within an expected, specific range. In addition, the offset frequencies of every laser could be maintained constant during scientific observation and even the whole mission cycle. The offset frequency can be positive or negative. To simplify the constraints, only the case of positive offset frequency is discussed. The mathematical model is as follows:

$$
\begin{aligned}
&\text{Max duration } t\\
&t = t\_\text{end} - t\_\text{start} + 1\\
&\tilde{f}_{12} = f_{12}(t\_\text{start}, t\_\text{end})\\
&\tilde{f}_{13} = f_{13}(t\_\text{start}, t\_\text{end})\\
&\tilde{f}_{23} = f_{23}(t\_\text{start}, t\_\text{end})\\
&s.t.\\
&\begin{cases}
LB <= \Delta f^1_{AB} <= UB\\
LB <= \Delta f^2_{CD} <= UB\\
LB <= \Delta f^3_{EF} <= UB\\
LB <= \Delta f^1_{AF} <= UB\\
LB <= \Delta f^1_{BC} <= UB\\
LB <= \Delta f^1_{AF} + 2\tilde{f}_{13} <= UB\\
LB <= \Delta f^1_{BC} + 2\tilde{f}_{12} <= UB\\
LB <= \Delta f^1_{AF} + \tilde{f}_{13} + \Delta f^3_{EF} + \tilde{f}_{23} - (\Delta f^1_{AB} + \Delta f^1_{BC} + \tilde{f}_{12} + \Delta f^2_{CD}) <= UB\\
LB <= \Delta f^1_{AF} + \tilde{f}_{13} + \Delta f^3_{EF} - (\Delta f^1_{AB} + \Delta f^1_{BC} + \tilde{f}_{12} + \Delta f^2_{CD} + \tilde{f}_{23}) <= UB
\end{cases}
\end{aligned}
\tag{5}
$$

where t is duration time, $t = t\_\text{start} - t\_\text{end} + 1$, and Max duration t is the goal. LB and UB represent the lower and upper bounds of the constraint, respectively. $f_{12}(t\_\text{start}, t\_\text{end})$, $f_{13}(t\_\text{start}, t\_\text{end})$, and $f_{23}(t\_\text{start}, t\_\text{end})$ are the time-varying Doppler shifts between each S/C from time t_start to time t_end, which are closely related to the orbit. The constraints are the functions of t_start and t_end. For example, if $t\_\text{start} = 1$ and $t\_\text{end} = 2$, the constraints could be expressed by Eq. (6) Δf^1_{AB}, Δf^2_{CD}, and Δf^3_{EF} should be constrained because they are the inner-spacecraft beats. Furthermore, Δf^1_{AF} and Δf^1_{BC} could be constrained; however, these constraints are not mandatory.

The flowchart of the implemented LP algorithm, as shown in Fig. 4, describes the solving process; the steps are as follows:

Step 1: Set $t\_\text{start} = 1$, and $t\_\text{end} = 1$.

Step 2: Set constraints according t_start and t_end.

Step 3: Solve the constraints equations established in Step 2 using the LP algorithm based on the interior point method [22].

Step 4: If the optimal solution is found, go to Step 5. Otherwise, go to Step 7.

Step 5: Save the solution of $t = t\_\text{start} - t\_\text{end} + 1$.

Step 6: If $t\_\text{end} = \text{EOF}$, go to Step 8. Otherwise, set $t\_\text{end} = t\_\text{end} + 1$, and go to Step 2.

Step 7: Set $t\_\text{start} = t\_\text{end}$, and go to Step 2.

Step 8: Optimization termination.

Finding a solution satisfying all constraints is the main task; thus, the optimization goal of the LP algorithm in Step 3 could be set to a constant. In Step 3, as long as a solution can satisfy all constraints, the process can reach Step 5, ensuring stability of the results. Therefore, the max duration time t could be found by the loop in Step 2 to Step 7. In particular, the LP algorithm is fast; it takes about 0.007 s to complete one loop of Step 2 to Step 7 by AMD Ryzen 9 3900X 12-Core Processor.

$$
\begin{cases}
LB <= \Delta f^1_{AB} <= UB\\
LB <= \Delta f^2_{CD} <= UB\\
LB <= \Delta f^3_{EF} <= UB\\
LB <= \Delta f^1_{AF} <= UB\\
LB <= \Delta f^1_{BC} <= UB\\
LB <= \Delta f^1_{AF} + 2f_{13}(1) <= UB\\
LB <= \Delta f^1_{BC} + 2f_{12}(1) <= UB\\
LB <= \Delta f^1_{AF} + f_{13}(1) + \Delta f^3_{EF} + f_{23}(1) - (\Delta f^1_{AB} + \Delta f^1_{BC} + f_{12}(1) + \Delta f^2_{CD}) <= UB\\
LB <= \Delta f^1_{AF} + f_{13}(1) + \Delta f^3_{EF} - (\Delta f^1_{AB} + \Delta f^1_{BC} + f_{12}(1) + \Delta f^2_{CD} + f_{23}(1)) <= UB\\
LB <= \Delta f^1_{AF} + 2f_{13}(2) <= UB\\
LB <= \Delta f^1_{BC} + 2f_{12}(2) <= UB\\
LB <= \Delta f^1_{AF} + f_{13}(2) + \Delta f^3_{EF} + f_{23}(2) - (\Delta f^1_{AB} + \Delta f^1_{BC} + f_{12}(2) + \Delta f^2_{CD}) <= UB\\
LB <= \Delta f^1_{AF} + f_{13}(2) + \Delta f^3_{EF} - (\Delta f^1_{AB} + \Delta f^1_{BC} + f_{12}(2) + \Delta f^2_{CD} + f_{23}(2)) <= UB
\end{cases}
\tag{6}
$$

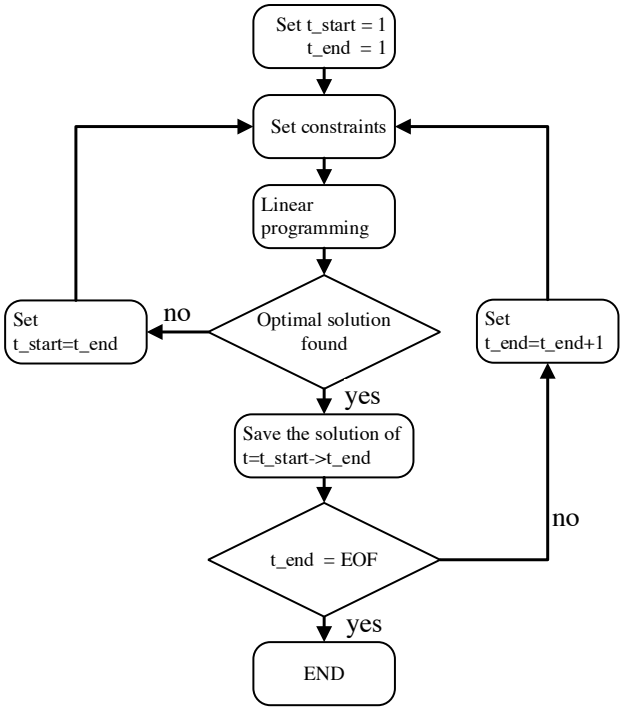

Fig. 4. LP algorithm flowchart.

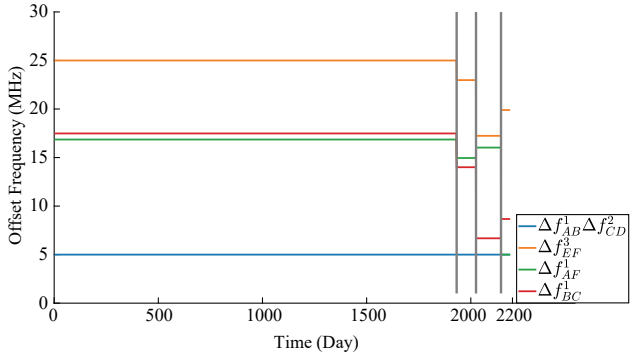

Fig. 5. Time-varying offset frequencies.

B. Offset Frequency Setting Results

The mission period of the Taiji program is six years or approximately 2190 days. The Doppler shifts $f_{12}(t)$, $f_{13}(t)$, and $f_{23}(t)$ can be calculated using the selected orbit [10]. By substituting $f_{12}(t)$, $f_{13}(t)$, and $f_{23}(t)$ into the above model and setting $LB = 5$ MHz and $UB = 25$ MHz, the results of the time-varying offset frequencies, shown in Fig. 5, can be calculated. Note that the entire process requires approximately 16 s. The x axis represents the day, while the y axis is the offset frequencies. Δf^1_{AB} and Δf^2_{CD} are the offset frequencies between two lasers in the same S/C, indicated by the blue line in the figure, which remain unchanged during the mission. The abscissa is divided into four areas using three gray vertical lines. The offset frequencies Δf^3_{EF} (orange line), Δf^1_{AF} (green line), and Δf^1_{BC} (red line) should be changed three times at these dividing lines to satisfy the frequency constraints during the task, which means that scientific observation will be interrupted three times.

Table 2. Offset Frequency Setting Strategy

Day	Δf^1_{AB} (MHz)	Δf^2_{CD} (MHz)	Δf^3_{EF} (MHz)	Δf^1_{AF} (MHz)	Δf^1_{BC} (MHz)	Duration (Days)
1–1931	5.00	5.00	25.00	16.86	17.48	1931
1932–2024	5.00	5.00	22.98	14.95	14.00	93
2025–2144	5.00	5.00	17.24	16.03	6.68	120
2145–2190	5.00	5.00	19.89	5.00	8.67	46

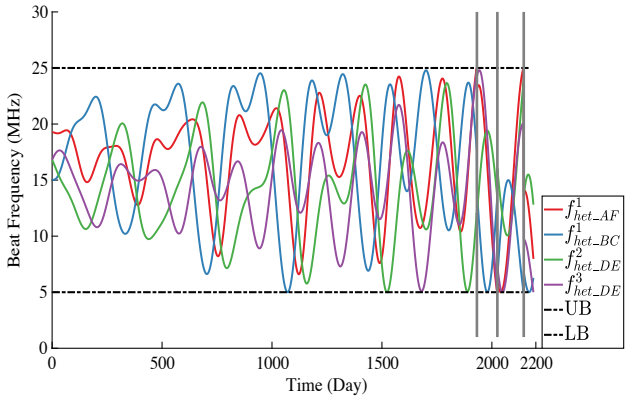

Fig. 6. Time-varying beat frequency. Black dotted lines represent the upper and lower bounds of the frequency constraint. Gray line is the dividing line.

The specific strategies used are listed in Table 2. The first column is the set values for the offset frequencies at different periods. Columns 2–6 represent the specific set values of Δf^1_{AB}, Δf^2_{CD}, Δf^3_{EF}, Δf^1_{AF}, and Δf^1_{BC}, respectively. Column 7 indicates the duration of each offset frequency. To prevent the beat frequency from exceeding the constraint interval, Δf^3_{EF}, Δf^1_{AF}, and Δf^1_{BC} must be changed on the 1932nd, 2025th, and 2145th day. Therefore, the maximum offset frequency duration is 1931 days, which substantially improves the results of Barke [11], for which the offset frequency can remain unchanged for up to 177 days.

Figure 6 shows the changes of the beat frequencies of the heterodyne interference for the entire mission after setting the offset frequencies. The black dotted lines represent the upper and lower bounds of the constraint, respectively. The beat frequency $f^1_{\text{het\_AF}}$, $f^1_{\text{het\_BC}}$, $f^3_{\text{het\_DE}}$, and $f^2_{\text{het\_DE}}$ are represented by the red, blue, green, and purple solid lines, respectively. The inter-spacecraft beat frequency was maintained within [5 MHz, 25 MHz] after being modulated by the offset frequency.

4. DISCUSSION

The main influencing factors of the frequency setting are the laser relative intensity noise, the bandwidth of the phase detector, and the Doppler shift between two S/Cs. This section focuses on the following factors: (1) the influence of relaxing and tightening the constraints on the offset frequency control strategies, i.e., the maximum duration of the offset frequencies under different upper and lower bounds; (2) the influence of Doppler shift oscillation amplitude on the frequency setting strategy.

A. Scaling of Upper and Lower Bounds

According to the previous analysis, the lower bound is determined by the relative intensity noise of the laser. For the Taiji program, the lower bound should be set to at least 1.5 MHz. The upper bounds of the constraints are directly related to the bandwidth of the phase detector. Using a phase detector with a larger detection bandwidth can increase the upper bounds, and vice versa, and reduce the upper limit.

To fully explore the strategies under different conditions, we scaled the upper and lower limits of the constraint until the maximum and minimum durations were reached. In our experiment, the value range of the lower bound was [3 MHz, 10 MHz], while the value range of the upper bound was [20 MHz, 27 MHz]. The maximum duration of the offset frequencies under different constraints are listed in Table 3.

In Table 3, LB and UB are the lower and upper bounds, respectively. The values in the table indicate that, when the constraints are tightened, the duration gradually decreases. For example, when the constraint is [6 MHz, 20 MHz], the feasible interval range is 15 MHz, and the longest duration is 668 days. When the constraints are [10 MHz, 21 MHz] and [10 MHz, 20 MHz], the feasible region is lower than 11 MHz; thus, it is necessary to change the offset frequencies every day. In contrast, when the constraints are [4 MHz, 27 MHz], [3 MHz, 26 MHz], and [3 MHz, 27 MHz], the duration is the longest. These results imply that the decisive factor for the longest duration is the scope of the feasible region. For example, when the feasible interval range is greater than or equal to 24 MHz, the offset frequencies need not be changed for the entire mission.

Table 3. Maximum Duration of Offset Frequencies by Different Constraints

	UB (MHz)							
LB (MHz)	**27**	**26**	**25**	**24**	**23**	**22**	**21**	**20**
3	2190	2190	2038	2030	1935	1058	1049	924
4	2190	2038	2030	1935	1058	1049	924	684
5	2038	2030	1931	1058	1049	924	684	675
6	1931	1561	1058	1049	847	684	675	668
7	1199	1058	847	769	683	668	418	297
8	847	769	683	668	418	297	280	173
9	683	668	418	297	280	173	115	82
10	418	297	280	173	115	82	1	1

Table 4. Change in Duration of the Offset Frequencies after Adding Multiple Factors[a]

	Cons (MHz)				
α	**[5,25]**	**[5,26]**	**[4,25]**	**[5,27]**	**[3,25]**
1	1931	2030	2030	2038	2038
0.99	1936	2031	2031	2040	2040
0.98	2026	2033	2033	2047	2047
0.97	2028	2034	2034	2190	2190
0.96	2029	2036	2036	2190	2190
0.95	2030	2039	2039	2190	2190
0.94	2032	2043	2043	2190	2190
0.93	2033	2190	2190	2190	2190
0.92	2035	2190	2190	2190	2190
0.91	2037	2190	2190	2190	2190
0.9	2040	2190	2190	2190	2190
0.89	2190	2190	2190	2190	2190

[a]Offset frequency setting plans that last the longest under different constraints and multiplier factors.

B. Doppler Shift

The relative velocity among the three S/Cs in the spacecraft constellation is the cause of the Doppler shift. Therefore, suppressing the relative velocity can further optimize the frequency setting strategy. In the currently selected orbit, the relative velocity varies with time, as shown in Fig. 7. To explore the influence of relative motion on the duration of offset frequencies, a multiple factor α is introduced to suppress the relative motion, as shown in Eq. (7):

$$\begin{cases} v_{12\_\mathrm{new}} = v_{12} \times \alpha \\ v_{13\_\mathrm{new}} = v_{13} \times \alpha \\ v_{23\_\mathrm{new}} = v_{23} \times \alpha \end{cases}. \tag{7}$$

In Eq. (7), v_{12}, v_{13} and v_{23} represent the relative velocities among the three S/Cs, and v_{12_new}, v_{13_new}, and v_{23_new} are the constrained results by α.

Simultaneously, the upper and lower bounds of the constraints are modified. The experimental results are summarized in Table 4.

In Table 4, α is the multiplier factor. "Cons" indicate the upper and lower bounds of the constraint. For example, [5,25] indicates that the lower and upper bounds are 5 and 25 MHz, respectively. Therefore, the feasible interval ranges corresponding to the constraints [5,25], [5,26], [4,25], [5,27], and [3,25] are 21, 22, 22, 23, and 23 MHz, respectively. The data in the table represent the maximum durations of the offset frequencies. The results in Table 4 demonstrate that the offset frequencies

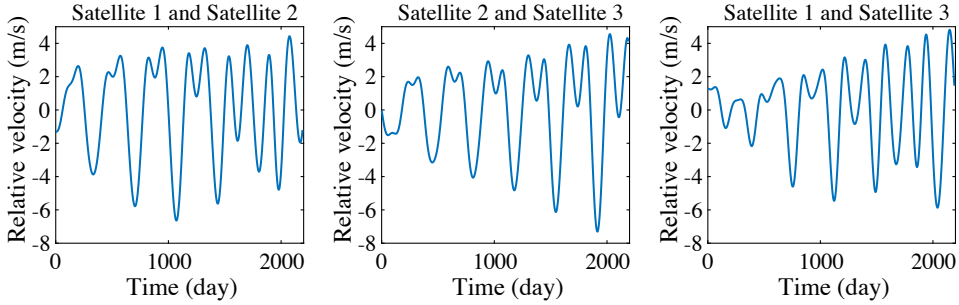

Fig. 7. Variation in the S/C's relative motion over time.

do not need to be changed during the mission using a suitable combination of adjustment factor α and constraints. For example, when the relative motion is reduced to 89% (maximum of 6.5 m/s) of the original with a feasible interval range of 22 MHz, the offset frequencies do not require change within six years. In Table 4, the offset frequency setting plans that can last the longest, under different constraints and multiplier factors, are indicated by a gray area. The above analysis shows that reducing the relative motion between the S/Cs or increasing the bandwidth of the phase detector can improve the maximum duration of the offset frequencies. The relative speed depends on the initial value of orbit determined by the deep space network. Bandwidth of the phase detector is limited by the design and processing level. On the premise of meeting the continuity of scientific measurement data, these factors need to be comprehensively considered to give the most reasonable offset frequency setting result.

Based on the above experimental results, there are two recommendations for the Taiji program to implement: 1) phase detectors with an upper bandwidth limit exceeding 26 MHz should be used, and the lower bound of beat frequencies should be set to be 4 MHz; 2) the relative speed between S/Cs will be constrained within 6.5 m/s by further improving the program's orbital constraints.

5. SUMMARY

In this study, the inter-spacecraft beat frequency setting problem was analyzed and solved for the Taiji program using the LP algorithm. The bandwidth of the phase detector determined the upper bound, and the lower bound depended on the relative intensity noise of the laser. For the frequency band of [5 MHz, 25 MHz], allowed in the Taiji program, the corresponding frequency allocation strategy was obtained. This strategy will allow the offset frequencies to remain unchanged for 1931 days.

Subsequently, the setting of the upper- and lower-frequency bounds was assessed. A scaling experiment for the upper and lower bounds of the detection range was conducted, and the longest durations of offset frequencies in a wide and narrow range were compared. Changing the offset frequencies every day is necessary when the feasible region is lower than 11 MHz. When the feasible interval range is greater than or equal to 24 MHz, the offset frequencies do not change during the mission. The influence of Doppler frequency shift was also analyzed. If the Doppler frequency shift could be restricted, it would benefit the frequency setting strategy. This method allows reaching the maximum duration using a suitable combination of adjustment factor α and frequency constraints. These results will provide a reference for parameter selection of the phase detector and further optimization of the orbit of the Taiji program.

In fact, outgoing laser light auxiliary functions like clock transfer should be considered. Sidebands for clock transfer is at the GHz level, which is not included in this paper. To establish a complete inter-spacecraft frequency distribution system for the Taiji program, this issue needs to be discussed in detail in follow-up work.

Funding. National Key Research and Development Program of China (2020YFC2200100); Chinese Academy of Sciences Strategic Pioneer Program on Space Science XDA1502110201.

Disclosures. The authors declare no conflict of interest.

Data Availability. Data underlying the results presented in this paper are not publicly available at this time but may be obtained from the authors upon reasonable request.

REFERENCES

1. W. R. Hu and Y. L. Wu, "Taiji program in space for gravitational wave physics and nature of gravity," Natl. Sci. Rev. **4**, 685–686 (2017).
2. A. Einstein and N. Rosen, "On gravitational waves," J. Franklin Inst. **223**, 43–54 (1937).
3. J. Weber, "Evidence for discovery of gravitational radiation," Phys. Rev. Lett. **22**, 1320–1324 (1969).
4. B. S. Sathyaprakash and B. F. Schutz, "Physics, astrophysics and cosmology with gravitational waves," Living Rev. Relativ. **12**, 1–141 (2009).
5. Z. Luo, Z. K. Guo, G. Jin, Y. Wu, and W. Hu, "A brief analysis to Taiji: science and technology," Results Phys. **16**, 102918 (2020).
6. C. Cutler and K. S. Thorne, "An overview of gravitational-wave sources," Gen. Relativ. Gravit. 72–111 (2002).
7. K. Danzmann, "LISA study team. LISA: laser interferometer space antenna for gravitational wave measurements," Classical Quantum Gravity **13**, A247 (1996).
8. A. Abramovici, W. E. Althouse, and R. W. Drever, "LIGO: the laser interferometer gravitational-wave observatory," Science **256**, 325–333 (1992).
9. W. M. Folkner, F. Hechler, T. H. Sweetser, M. A. Vincent, and P. L. Bender, "LISA orbit selection and stability," Classical Quantum Gravity **14**, 1405–1410 (1997).
10. W.-L. Tang, *Preliminary Study of the Orbit Design of the Chinese Mission to Detect the Gravitational Wave in Space* (Chinese Academy of Sciences University, 2014).
11. S. Barke, *Inter-Spacecraft Frequency Distribution for Future Gravitational Wave Observatories* (Gottfried Wilhelm Leibniz Universität Hannover, 2015).
12. P. W. McNamara, "Weak-light phase locking for LISA," Classical Quantum Gravity **22**, S243–S247 (2005).
13. M. Tröbs, S. Barke, J. Möbius, M. Engelbrecht, D. Kracht, L. d'Arcio, G. Heinzel, and K. Danzmann, "Lasers for LISA: overview and phase characteristics," J. Phys. Conf. Series **154**, 012016 (2009).
14. G. Hechenblaikner, R. Gerndt, U. Johann, P. Luetzow-Wentzky, V. Wand, H. Audley, K. Danzmann, A. Garcia-Marin, G. Heinzel, M. Nofrarias, and F. Steier, "Coupling characterization and noise studies of the optical metrology system onboard the LISA Pathfinder mission," Appl. Opt. **49**, 5665–5677 (2010).
15. K. Danzmann, T. A. Prince, P. Binetruy, *et al.*, "LISA: unveiling a hidden universe," Assessment Study Report ESA/SRE 3(2) (2011).
16. P. Amaro-Seoane, S. Aoudia, S. Babak, *et al.*, "eLISA: astrophysics and cosmology in the millihertz regime," arxiv:1201.3621 (2012).
17. R. Zhu, J. Zhou, J. Liu, D. Chen, Y. Yang, and W. Chen, "Solid state tunable single-frequency laser based on non-planar ring oscillator," Chin. J. Laser **38**, 70–75 (2011).
18. K. Danzmann, "LISA mission overview," Adv. Space Res. **25**, 1129–1136 (2000).
19. P. McNamara, S. Vitale, and K. Danzmann, "Lisa pathfinder," Classical Quantum Gravity **25**, 114034 (2008).
20. G. Müller, P. McNamara, I. Thorpe, and J. Camp, "Laser frequency stabilization for LISA," NASA technical publication TP-2005–212790 (2005).
21. V. Leonhardt and J. B. Camp, "Space interferometry application of laser frequency stabilization with molecular iodine," Appl. Opt. **45**, 4142–4146 (2006).
22. S. Mehrotra, "On the implementation of a primal-dual interior point method," SIAM J. Optim. **2**, 575–601 (1992).